Multidisciplinary Cancer Investigation Original Article

July 2023, Volume 7, Issue 3

Cumulative Effect of a Gold-Poly(o-aminophenol) Nanocomposite and Doxorubicin in Photothermal Therapy, Sonodynamic Therapy, and Chemotherapy of Breast Cancer (MCF-7 Cell Line)

Paria Tamaddon[1,2], Ghazale Perota[2], Rezvan Dehdari Vais[2], Naghmeh Sattarahmady[1,2*]

[1] Department of Medical Physics, School of Medicine, Shiraz University of Medical Sciences, Shiraz, Iran

[2] Nanomedicine and Nanobiology Research Center, Shiraz University of Medical Sciences, Shiraz, Iran

**Corresponding author: Naghmeh Sattarahmady, Department of Medical Physics, School of Medicine, Shiraz University of Medical Sciences, Shiraz, Iran. Tel: +987132349332; Fax: +987132349332. E-mail: sattarahmady@yahoo.com; nsattar@sums.ac.ir*

Submitted: 28 January 2023

Revised: 18 June 2023

Accepted: 29 June 2023

Published: 12 July 2023

Keywords:
Lasers, Semiconductor
Ultrasonic Waves
Drug Delivery Systems
2-aminophenol

Introduction: Nowadays, the applications of non-invasive treating cancer methods such as photothermal therapy (PTT) and sonodynamic therapy (SDT) are increasing. These treatments use photo/sonosensitizers, which are activated after being exposed by laser light irradiation and ultrasound (US) exposure, respectively.

Methods: Herein, a gold-poly (ortho-aminophenol) nanocomposite (Au-PoAP NC) with a spherical shape, a diameter of 46±8 nm was synthesized and evaluated as an 808-nm laser photosensitizer (with 30% photothermal efficiency) and a sonosensitizer upon US exposure. Additionally, Au-PoAP NC was appraised with doxorubicin (as a chemotherapy agent) for treating breast cancer cells. The MTT test was done for cell-toxicity evaluation of Au-PoAP NC, doxorubicin, and Au-PoAP NC with doxorubicin with or without irradiation and US exposure (separately and synchronously).

Results: The results proved that light irradiation and US exposure (separately and synchronously) of Au-PoAP NC with doxorubicin significantly enhanced the cell toxicity in other treatment groups. Moreover, cytotoxicity of Au-PoAP NC, doxorubicin, and Au-PoAP NC with doxorubicin toward MCF-7 cells upon PTT and/or SDT was investigated from the aspect of reactive oxygen species (ROS) formation. Calculating the combination indices revealed that synchronous administration of Au-PoAP NC and doxorubicin and light irradiation and US exposure represented a synergistic therapeutic manner for treating cancer cells.

Conclusion: This study proved that the synchronous combination of PTT and SDT using Au-PoAP NC with doxorubicin would be an exemplary approach for treating the breast cancer cell line of MCF-7.

INTRODUCTION

Cancer is the uncontrolled proliferation of cells and their spread to other body parts [1]. Worldwide, breast cancer is the second dominant reason of cancer-related deaths among women [2]. Some common cancer treatments such as surgery, chemotherapy, radiotherapy, or a combination of these modalities include side effects, low precision, high risks, and less patient satisfaction. In recent years, scientists

[DOI: 10.61186/mci.7.3.9]

developed therapies to minimize side effects, maximize effectiveness and safety, and affordable treatments [3-5]. Phototherapy and sonodynamic therapy (SDT) are new cancer treatments. Phototherapy includes two categories: photothermal therapy (PTT) and photodynamic therapy (PDT). PTT involves near-infrared laser (NIR) radiation that has a wavelength between 700-1000 nm, and light-absorbing non-toxic chemical agents, called photosensitizers, penetrate deep into the targeted tissues (at least 10 cm) to treat cancer [6]. SDT is not only a non-invasive, inexpensive, and non-ionizing treatment but also has a deeper penetration. This treatment uses low-intensity ultrasound (US) waves (0.5-5 W cm-2) and sonosensitizers, non-toxic sensitizing chemical agents [7, 8]. Ultrasound (US) waves are safer due to their non-ionizing nature and low-tissue weakening without energy loss. They penetrate the body tissues to a great extent and focus at a certain depth on the cancerous tumors [9, 10]. US waves create heat according to the duration of radiation, intensity, and frequency. Additionally, they deposit different thermal and non-thermal effects on body tissues. Hence, they cause cancer cell death by creating toxicity, generating heat and pore-making processes by sonosensitizers through creating reactive oxygen species (ROS) in tumor tissues [7, 8, 11]. The most crucial advantage of SDT over PTT is the ability of US waves to focus on malignant tumors located within deep tissues. It has the least destructive effect on adjacent healthy tissues. Besides, SDT is a reasonable treatment [7, 8]. So far, nanoparticles based on gold, copper [12], ferrite [13, 14], silver [15, 16], silica [17, 18], titania [19, 20], and liposomes [21, 22] have emerged as influential sensitizers in PTT and SDT due to their unique optical, chemical properties, and suitable size [23]. Among these nanoparticles, gold nanoparticles (AuNPs) have great potential for cancer diagnosis and treatment due to their unique local surface plasmon resonance (LSPR), light scattering, absorption potential, facile synthesis, and surface modification ability [3, 24-27]. AuNPs with different shapes, sizes, conjugations, and coatings were used as PTT and SDT sensitizers [6, 28] and delivery of numerous anti-cancer drugs [29-31]. Meanwhile, conjugation that influences the properties of AuNPs has been one of the essential issues for the diagnosis and treatment aims of AuNPs applications [32-35].

Doxorubicin is a cytotoxic antibiotic used to treat a variety of hematopoietic malignancies and solid tumors in breast [36], ovarian [37], lung [38], gastric [39], and thyroid cancers [40]. The mechanism of action of doxorubicin is to break down strands of DNA, which then inhibits topoisomerase II, disrupts mitochondria, causes formation of free radicals, and intensifies oxidative stress damage [41]. Although doxorubicin is very effective with a short half-life of 5 min, its doses must be carefully and correctly selected due to some side effects [42]. In the current investigation, a gold-poly (ortho-aminophenol) (PoAP) nanocomposite (Au-PoAP NC) was synthesized. Properties of Au-PoAP NC were then evaluated in terms of capabilities as a photosensitizer for 808-nm laser light irradiation, sonosensitizer for US exposure, promoter for doxorubicin effectiveness, and stimulator for intracellular ROS generation. Au-PoAP NC represented an effective dual sensitizing function in synchronous photothermal therapy and sonodynamic therapy (PTT/SDT) with doxorubicin for annihilating in vitro breast cancer.

METHODS

All chemical compounds were acquired from Scharlau Chemie Co. (Spain), Merck Co. (Germany), or Sigma Chemicals Co. (USA). The chemicals were utilized in the absence of any pre-purification, and deionized water (DIW) was applied all over the investigation.

Synthesis and Characterization of Au-PoAP NC

0.15 g ortho-aminophenol was first dissolved in 10 mL of 1.0 mol L^{-1} hydrochloric acid. Afterward, 0.18 g of ammonium persulfate was dissolved in 10 mL of 1.0 mol L^{-1} hydrochloric acid. Next, the two mentioned solutions were mixed and left in a shaker for 2 h. Then, the suspension was kept at 25 °C for 48 h. Subsequently, it was centrifuged for 6 min at 6000 rpm, and each time the suspended liquid was discarded, the precipitate was washed with 40 mL of DIW until it became colorless. Later, the sediment was rinsed twice with 50 mL of 0.10 mol L^{-1} ammonia and centrifuged again. After that, the sediment was suspended in 30 mL of DIW and left at 25 °C for 24 h. Then, 360 µL of HAuCl4 solution was solved in 10 mL of PoAP suspension and left in a shaker for 2 h. It was then centrifuged for 6 min at 6000 rpm. Eventually, the suspended liquid was

[DOI: 10.61186/mci.7.3.9]

thrown away, and the precipitate was re-suspended in 2.0 mL of DIW. To record UV-vis absorption spectra of Au-PoAP NC, the Rayleigh double beam spectrophotometer (China) was used. Au-PoAP NC morphology and size were appraised by field emission scanning electron microscopy (FESEM) using a TESCAN Mira 3-XMU (Czech Republic) with the capability of energy dispersive X-ray (EDX) analysis. The hydrodynamic dimensions, along with the distribution of Au-PoAP NC, was also measured by dynamic light scattering using a particle size analyzer of Scatterscope I, Qudix (Korea). The Zeta potential of Au-PoAP NC was measured by a Malvern Nano-ZS ZEN 3600 (UK).

Cell Line Preparation

A human mammary breast tumor MCF-7 cell line was purchased from the Pasteur Institute of Iran and cultured in Roswell Park Memorial Institute-1640 (RPMI) medium, which contains 1% antibiotics (penicillin/streptomycin, 10,000 µg mL-1) and 10% fetal bovine serum (FBS) in a humidified atmosphere comprising 5% CO2 at 37 °C cell incubator. Cell incubator conditions of 5% CO2 at 37 °C were followed throughout the study.

MCF-7 Cytotoxicity Assessment in the Presence of Au-PoAP NC or Doxorubicin

MCF-7 cells were cultured in 96-well culture plates and incubated for 24 h to adhere to the wells. Afterward, the cells were treated with different concentrations of Au-PoAP NC (0 to 50 µg mL-1) or doxorubicin (0 to 1.7 µg mL^{-1}). In the next 24 h, the cytotoxicity of Au-PoAP NC and doxorubicin were individually measured by the MTT (3-(4,5-dimethylthiazol-2-yl)-2,5-diphenyl-tetrazolium bromide) assay. The optical intensity of each well was recorded at 570 nm using a microplate reader of Stat Fax (USA). Untreated cells were selected as controls. All measurements for each concentration were examined in three times. After measuring 50% inhibitory concentration (IC50) for Au-PoAP NC and doxorubicin, MCF-7 cells were synchronously treated with IC50 of Au-PoAP NC (5.0 µg mL^{-1}, vide infra, section 3) and doxorubicin (0.58 µg mL^{-1}, vide infra, section 3) to investigate their synchronous effect. After 24 h of incubation, the cytotoxicity was estimated by the MTT assay. Untreated cells were selected as a control. All measurements were executed in triplicate.

Diode Laser and Ultrasound Measuring Devices

An 808 nm-diode laser pursued with a power of 1000 mW from Thorlabs (Germany) was employed. This system was supplied with a temperature checkout. A power density of 1.0 W cm-2 was set. For PTT, light irradiation was always implemented on 96-well cell culture plates for 10 min. The ultrasonic instrument from Novin (Iran) worked at a frequency of 1.0 MHz, a power density of 1.0 W cm-2, and a duty ratio of 10% throughout the study. The transducer surface of the instrument was shielded with an ultrasonic gel and placed under the culture plate. Moreover, it was always exposed to US waves for 10 min.

Experimental Set Up for Estimation of Photo-thermal Conversion Efficiency (η) of Au-PoAP NC

A time constant method was employed to calculate η [43]. Equipments needed for this calculation were a 1.5 mL glass cuvette that contained an Au-PoAP NC suspension (100 µg mL^{-1}) and a thermoprobe of Lutron (Taiwan), which was kept away from the laser beam. This thermoprobe had a precision of 0.01°C and recorded temperature fluctuations with time. The Au-PoAP NC suspension was first irradiated by laser light, while temperature changes were recorded until reaching a stabilization. Then, the laser was turned off, and recording temperature changes were continued until reaching the starting value.

Separate and Synchronous Evaluation PTT, SDT or PTT/SDT of MCF-7 Cells Using Au-PoAP NC and/or Doxorubicin

24 h post-seeding, in vitro PTT, SDT, or PTT/SDT of MCF-7 cells using Au-PoAP NC or doxorubicin, and a combination of Au-PoAP NC and doxorubicin on MCF-7 cells were pursued by the MTT test. Cells were segregated into the following groups:

In the group of Ctrl (control group), cells were incubated for 24 h without any treatment followed by the MTT test.

In groups of NC^+, Dox^+, NC^+Dox^+, P^+, S^+ and P^+S^+ (neither PTT nor SDT groups), cells were treated with IC50 of Au-PoAP NC, with IC50 of doxorubicin, with IC50s of Au-PoAP NC and IC50 of doxorubicin synchronously, with laser light, with US waves, and with laser light followed by US

[DOI: 10.61186/mci.7.3.9]

waves, respectively. After cell incubation for 24 h, the MTT test was carried out.

In groups of NC^+P^+, Dox^+P^+, and $NC^+Dox^+P^+$ (PTT groups), cells were treated with IC50s of Au-PoAP NC and doxorubicin separately or synchronously, incubated for 3 h, then laser light was irradiated, and ultimately incubated for 21 h. These steps were followed by the MTT assay.

In groups of NC^+S^+, Dox^+S^+, and $NC^+Dox^+S^+$ (SDT groups), cells were treated with IC50s of Au-PoAP NC and doxorubicin separately or synchronously, incubated for 3 h, then US waves were exposed, and ultimately incubated for 21 h. These steps were followed by the MTT assay.

In groups of $NC^+P^+S^+$, $Dox^+P^+S^+$, and $NC^+Dox^+P^+S^+$ (PTT/SDT groups), cells were treated with IC50s of Au-PoAP NC and doxorubicin separately or synchronously, incubated for 3 h, laser light was irradiated, then US waves were exposed, and ultimately incubated for 21 h. These steps were followed by the MTT assay.

Detection of Intracellular ROS Generation in MCF-7 Cells

24 h post-seeding, in vitro PTT, SDT, or PTT/SDT of MCF-7 cells using Au-PoAP NC or doxorubicin, and a combination of Au-PoAP NC and doxorubicin on MCF-7 cells were pursued for the detection of intracellular ROS generation. Fluorescence intensity (F.I.) of 2',7'-dichlorodihydrofluorescein diacetate (DCFH-DA) was recorded as a sign of intracellular ROS generation. Cells were segregated into different groups based on the previous section. Adding Au-PoAP NC and doxorubicin, laser light irradiation, and US wave exposure were done based on the previous section. After 2.5 h incubation of the cells, 100 μL of a fresh DCHF-DA solution (50 $\mu mol\ L^{-1}$) was inserted into each sample. Then, after 30 min, the cells were rinsed three times with phosphate buffer saline (20 $mmol\ L^{-1}$, pH=7.4, PBS), and 100 μL of a lysis buffer (mixture of NaCl, Triton X-100, Tris-HCl, pH=8.0) was added to each sample. After 30 min, fluorescence intensity (FI) at 520 nm was ultimately recorded upon excitation at 485 nm within 96-well black plates using a microplate reader of Biotek (USA). Adding Au-PoAP NC and doxorubicin, laser light irradiation, and US wave exposure were done based on the previous section.

Au-PoAP NC Uptake in MCF-7 Cells

24 h post-seeding MCF-7 cells were treated with IC50 of Au-PoAP NC. After incubation for 24 h, the cells were rinsed with PBS three times, lysed, and digested with aqua regia. The amount of Au-PoAP NC uptake was then recorded by inductively coupled plasma optical emission spectrometry (ICP-OES). using a Varian 730-ES (USA).

Estimation of Domination of Synergism Results

Domination of synergism effects during treatments of MCF-7 cells of PTT (separate and synchronous combinations of Au-PoAP NC, doxorubicin and light irradiation), SDT (separate and synchronous combination of Au-PoAP NC, doxorubicin and US exposure), and PTT/SDT (synchronous combination of Au-PoAP NC, doxorubicin, light irradiation and US exposure) was evaluated by calculation of combination indices (CIs). When two factors A and B separately or synchronously affect cell toxicity [44]:

Equation 1:

$$CI=(100-T_A)\times(100-T_B)/(100-T_{AB})$$

Where T_A and T_B are the percent of cell toxicities induced by effects of A and B factors, and T_{AB} is the percent of cell toxicity induced by synchronous effect of A and B factors. The values of CI more, equal or less than one designates domination of synergism, additive, or antagonism consequences, respectively. For the present study, four agents of NC^+, Dox^+, P^+, and S^+ independently and/or synchronously affected the cell toxicity. CIs were first calculated in the specified order of administration between each pairwise (combination effects of NC^+ with Dox^+, P^+ or S^+, and Dox^+ with P^+ or S^+). If CI was portended domination of synergistic effect in a pairwise combination, the corresponding factors were considered as a new single factor, and a new combination index was calculated for combination with a third factor. The combination effect of NC and Dox with P and S was measured alike (presuming each one as a single agent).

Statistical Analysis

More than three parallel evaluations were conducted to measure each quantity. Kruskal-Wallis with Dunn's as the post hoc test and independent t-test were performed to analyze the statistical significance of the results using GraphPad (Prism 6) software. P<0.05 were considered statistically significant.

[DOI: 10.61186/mci.7.3.9]

RESULTS

It has been revealed that AuNPs have the potential to be used as photosensitizers and sonosensitizers in PTT and SDT, respectively [6, 24, 26-28, 30]. On the other hand, doxorubicin is one of the approved drugs for treating breast adenocarcinoma [36]. Application of Au-PoAP NC, doxorubicin, PTT, and SDT would be an effective and impressive route for the treatment of MCF-7 cells and a new way for facilitated drug delivery.

Characterization of Au-PoAP NC

Figure 1 shows UV-vis absorption spectra of the as-synthesized Au-PoAP NC and after six months of storage at room temperature in DIW and a photograph from Au-PoAP NC. The spectra contained peaks at 422 and 214 nm and a shoulder at around 512 nm. The former peaks were derived from the inherent absorption of PoAP, and the latter shoulder was due to the LSPR effect of gold. Au-PoAP NC also had absorption at the 850-900 nm range, indicating that it could act as a proper photosensitizer in PTT upon 808 nm laser light activation. Furthermore, there was a minor difference between the spectra, deducing that Au-PoAP NC had good stability.

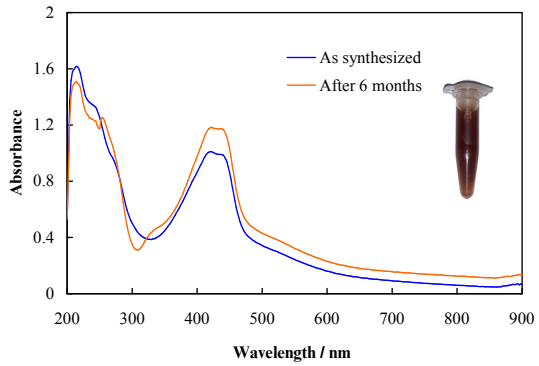

Figure 1: UV-vis Spectra of the As-Synthesized Au-PoAP NC After 6 Months of Storage and a Photograph From Au-PoAP NC (Inset)

Figure 2A shows a FESEM image of Au-PoAP NC showing porous nanoparticles of 46±8 nm. The hydrodynamic size of Au-PoAP NC was also obtained to be 48 nm with a span value of 0.9, indicating a narrow size distribution. Recent studies have shown that sub-50 nm-sized nanostructures can penetrate more effectually into tumor tissues. In addition, they can be excreted promptly across renal filtration, compared to the larger-sized nanostructures (50-100 nm) [45, 46]. An EDX spectrum of Au-PoAP NC is also presented in Figure 2B, indicating elemental purity with a weight percent of 10.6% for gold in Au-PoAP NC. The Zeta potential of Au-PoAP NC was -26±2 mV. The amount of Au-PoAP NC that uptakes over 24 h into MCF7 cells (uptake level in NC^{+} cell groups) was obtained as 5.76 ng $cell^{-1}$.

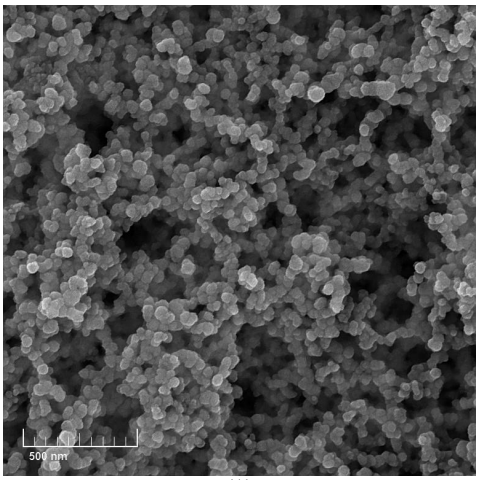

(A)

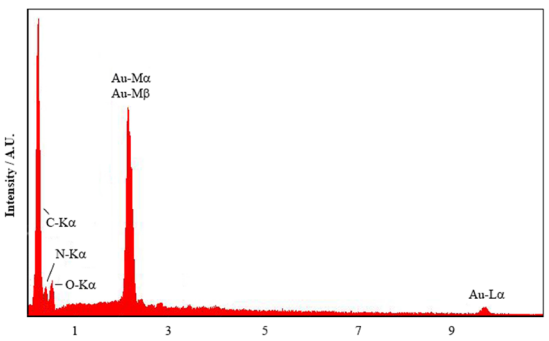

Element	Weight percent
C	63.1
N	12.3
O	14.0
Au	10.6

(B)

Figure 2: A FESEM Image of Au-PoAP NC

Calculation of η

η was measured based on a time constant method to evaluate the thermal efficiency of Au-PoAP NC [43]. The balancing energy in Au-PoAP NC can be expressed as [43]:

Equation 2:

$$Q_{\text{Au-PoAP NC}}+Q_{diss}=Q_{surr}+\Sigma m_i C_{Pi}\,(dT/dt)$$

Where, QAu-PoAP NC, Qdiss and Qsurr are the inputted energy by Au-PoAP NC, absorbed energy by

the cuvette and solvent (in the absence of Au-PoAP NC), and heat dissipation away from the system, respectively. Furthermore, m, CP, T, and t are the water mass, heat capacity of water, solution temperature, and elapsed time of light irradiation, respectively. QAu-PoAP NC and Qsurr are defined as:

Equation 3:

$$Q_{Au\text{-}PoAP\ NC}=(1 - 10^{-A_{\lambda}})\ I\eta$$

Equation 4:

$$Q_{surr}=(T - T_{surr})hS$$

Where A_{λ}, I, T_{surr}, h, and S are absorbance at 808 nm, laser input power, ambient temperature, heat transfer coefficient, and surface area of light radiation, respectively. Q_{diss} was obtained as 7.1 mW. While the input and output heat became equal, T reached a maximum value, and accordingly:

Equation 5:

$$Q_{Au\text{-}PoAP\ NC}+Q_{diss}=Q_{surr\text{-}max}=(T_{max}-T_{surr})hS$$

Where T_{max} and $Q_{surr\text{-}max}$ are the highest constant temperature and heat dissipation away from the system at T_{max}, respectively. Using equations 2 to5 , η will be:

Equation 6:

$$\eta= [hS\ (Tmax - Tsurr) - Qdiss] / [I\ (1 - 10_{-A})]$$

hS was measured while the light source was switched off, and the temperature decreased (cooling curve). θ and τ are dimensionless temperature and time constant, respectively, and are obtained from the cooling diagram. θ and τ are describe as:

Equation 7:

$$\theta=(T-T_{surr})/(T_{max}-T_{surr})$$

Equation 8:

$$hS=\Sigma mC_p/\tau$$

By replacement equations 7 and 8 in equation 2:

Equation 9:

$$d\theta/dt=1/\tau\{\theta-[(Q_{Au\text{-}PoAP\ NC}+Q_{diss})/hS(T_{max}-T_{surr})]$$

After switching off the laser:

Equation 10:

$$Q_{Au\text{-}PoAP\ NC}+Q_{diss}=0$$

Hence, equation 9 becomes:

Equation 11:

$$d\theta/dt = -\theta/t$$

And after integration,

Equation 12:

$$t=-\tau ln\theta$$

Accordingly, τ is stated as the slope of a cooling curve.

Figure 3A indicates temperature changes of 100 µg mL^{-1} Au-PoAP NC suspension (100 µg mL^{-1}) in DIW associated with heating upon light irradiation at 808 nm with a fixed output power density of 1.0 W cm^{-2} followed by switching off the light source and releasing to cool down. Laser switching on led to a maximum value (T_{max}, heating curve), and upon switching off, temperature decrement to room temperature was followed (cooling curve). Using the data presented in the Figure, T_{max} as 7.2 °C and the relation of t to -ln θ (Figure 3B) from the cooling curve were obtained. Using Figure 3B, hS was 4.73 mW. Using this value, absorption of 100 µg mL^{-1} Au-PoAP NC at 808 nm (≅0.36), and equation 6, a value of 30.2% was attained for η.

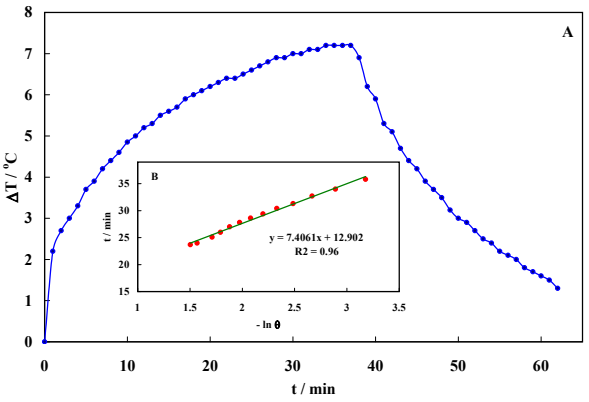

Figure 3: A) temperature changes of a 100 µg mL^{-1} Au-PoAP NC suspension in DIW associated with heating upon light irradiation at 808 nm with a fixed output power density of 1.0 W cm^{-2} following by switching off the light source and releasing to cool down; B) Dependency of t on -ln θ that was derived from the cooling part of the curve presented in Figure 3A

MCF-7 Cytotoxicity

The cytotoxicity effect of Au-PoAP NC, doxorubicin, and Au-PoAP NC with doxorubicin upon light irradiation, US exposure, and their combination was determined by the MTT test separately and

[DOI: 10.61186/mci.7.3.9]

synchronously under in vitro conditions. Figure 4A shows the cell toxicity effect of Au-PoAP NC on MCF-7 cells, representing increment in the cytotoxicity upon an increment in the Au-PoAP NC concentration 24 h after treatment without any irradiation. The results indicated that Au-PoAP NC at low concentrations is biocompatible, e.g., cytotoxicity was <20% at 0.5 µg mL^{-1} Au-PoAP NC. In addition, an IC50 value of 5.0 µg mL^{-1} was calculated for Au-PoAP NC toward MCF-7 cells. Au-PoAP NC (46 nm) was highly smaller than MCF-7 cells (8 µm) and could easily enter the cells to induce necrosis [47]. Figure 4B shows and compares the cytotoxicity effects of laser light (P^+), US waves (S^+), laser light/US waves (P^+S^+), Au-PoAP NC (NC^+), and Au-PoAP NC upon PTT (NC^+P^+), SDT (NC^+S^+), and PTT/SDT ($NC^+P^+S^+$). The results indicated that both laser light and US waves induced cytotoxicity with a deeper effect from light and an additive effect from synchronous treatment. While Au-PoAP NC alone was more effective than both separate or synchronous light and US to kill the cells, PTT, SDT, and PTT/SDT using Au-PoAP NC provided drastic effect. Quantitatively, PTT, and SDT using Au-PoAP NC enhanced cytotoxicities by 60 and 57%, respectively, compared to Ctrl. In addition, PTT/SDT using Au-PoAP NC enhanced cytotoxicity by 66%, compared to Ctrl. CIs for the combined treatments were also obtained as 1.11, 1.15, and 1.20 for NC^+P^+, NC^+S^+, and $NC^+P^+S^+$ groups, respectively. All CIs were greater than unity, revealing that synergism effects were predominant, and the highest effectiveness was PTT/SDT using Au-PoAP NC.

Figure 5A shows the cell toxicity effect of doxorubicin on MCF-7 cells, representing an increment in the cytotoxicity upon increment in the doxorubicin concentration 24 h after treatment without any irradiation. An IC50 value of 0.58 µg mL^{-1} was obtained for doxorubicin toward MCF-7 cells, which was in agreement with the other study [48]. Anticancer activity of doxorubicin arises from the ability to break the strands of DNA, inhibit topoisomerase II, and disrupt cellular mitochondria (which increases mitochondrial fragmentation). These lead to the formation of free radicals, which intensify oxidative stress damage and eventually cause apoptosis [49]. Doxorubicin can also fight tumors by controlling intramembrane proteolysis, which triggers the cleavage of membrane-bound proteins. This cleavage releases soluble messenger molecules that ultimately lead to apoptosis [50]. Figure 5B shows and compares the cytotoxic effect produced by laser light (P+), US waves (S+), laser light/US waves (P+S+), doxorubicin (Dox+), and doxorubicin upon PTT (Dox+P+), SDT (Dox+S^+), and PTT/SDT ($Dox^+P^+S^+$). The results indicated that while doxorubicin alone was more effective than separate and synchronous light and US to kill the cells, PTT, SDT, and PTT/SDT using doxorubicin provided drastic effect. Quantitatively, PTT and SDT using doxorubicin enhanced cytotoxicities by 64 and 58%, respectively, compared to Ctrl. In addition, PTT/SDT using doxorubicin enhanced cytotoxicity by 79%, compared to Ctrl. CIs for the combined treatments were also obtained as 1.18,

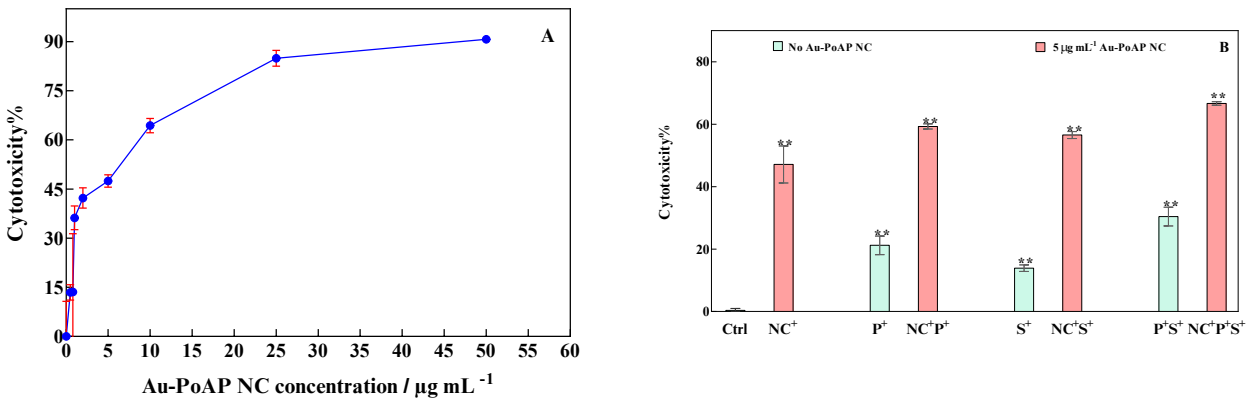

Figure 4: A) Cytotoxicity effect of Au-PoAP NC on MCF-7 cells with different concentrations without any radiation; B) Cytotoxicity effects of control (Ctrl), laser light (P^+), US waves (S^+), laser light/US waves (P^+S^+), Au-PoAP NC of 5 µg mL^{-1} (NC^+), and Au-PoAP NC of 5 µg mL^{-1} upon PTT (NC^+P^+), SDT (NC^+S^+) and PTT/SDT ($NC^+P^+S^+$) toward MCF-7 cells
Cytotoxicity in all groups had significant differences (**) with control group, and statistical significant differences (**) between the cytotoxicity in all possible pairwise are indicated (P<0.001).

[DOI: 10.61186/mci.7.3.9]

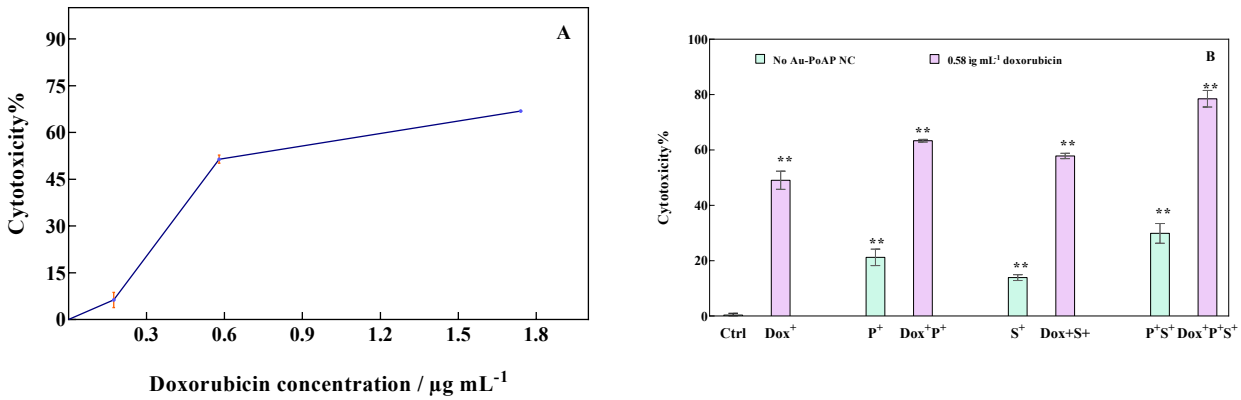

Figure 5: A) Cytotoxicity effect of doxorubicin on MCF-7 cells with different concentrations without any radiation; B) Cytotoxicity effects of control (Ctrl), laser light (P^+), US waves (S^+), laser light/US waves (P^+S^+), doxorubicin of 0.58 μg mL^{-1} (Dox^+), and doxorubicin of 0.58 μg mL^{-1} upon PTT (Dox^+P^+), SDT (Dox^+S^+) and PTT/SDT ($Dox^+P^+S^+$) toward MCF-7 cells
Cytotoxicity in all groups had significant differences (**) with control group, and statistical significant differences (**) between the cytotoxicity in all possible pairwise are indicated ($P<0.001$).

1.12, and 1.66 for the Dox^+P^+, Dox^+S^+, and $Dox^+P^+S^+$ groups, respectively. All CIs were greater than unity, revealing that synergism effects were predominant, and the highest effectiveness was PTT/SDT using Au-PoAP NC.

Figure 6 shows and compares synchronous cytotoxicity effects of laser light (P^+), US waves (S^+), laser light/US waves (P^+S^+), and Au-PoAP NC with doxorubicin (NC^+Dox^+) upon PTT ($NC^+Dox^+P^+$), SDT ($NC^+Dox^+S^+$), and PTT/SDT ($NC^+Dox^+P^+S^+$). The results indicated that while Au-PoAP NC with doxorubicin was more effective than separate and synchronous light and US to kill the cells, PTT, SDT, and PTT/SDT using Au-PoAP NC with doxorubicin provided drastic effect. Quantitatively, PTT and SDT using Au-PoAP NC with doxorubicin enhanced cytotoxicities by 83 and 80%, respectively, compared to Ctrl. In addition, PTT/SDT using Au-PoAP NC with doxorubicin enhanced cytotoxicity by 89%, compared to Ctrl. Therefore, Au-PoAP NC with doxorubicin demonstrated a more toxic effect (75% cytotoxicity, Figure 6) than Au-PoAP NC (42% cytotoxicity, Figure 4B) and doxorubicin (46% cytotoxicity, Figure 5B), separately. These results proved the cumulative effect of Au-PoAP NC and doxorubicin in PTT, SDT, and chemotherapy of MCF-7 cells and the crucial role of Au-PoAP NC for facilitated doxorubicin delivery. CIs for these treatments were also obtained as 1.34, 1.33, and 1.52 for the $NC^+Dox^+P^+$, $NC^+Dox^+S^+$, and $NC^+Dox^+P^+S^+$ groups, respectively. All CIs were greater than unity, revealing that synergism effects were predominant, and the highest effectiveness treatment among all the treatments presented was from PTT/SDT using Au-PoAP NC with doxorubicin.

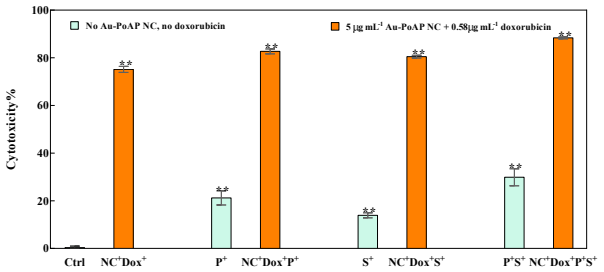

Figure 7: Synchronous cytotoxicity effects of laser light (P^+), US waves (S^+), laser light/US waves (P^+S^+), and Au-PoAP NC of 5 μg mL^{-1} with doxorubicin of 0.58 μg mL^{-1} (NC^+Dox^+) upon PTT ($NC^+Dox^+P^+$), SDT ($NC^+Dox^+S^+$) and PTT/SDT ($NC^+Dox^+P^+S^+$)
Cytotoxicity in all groups had significant differences (**) with control group, and statistical significant differences (**) between the cytotoxicity in all possible pairwise are indicated ($P<0.001$).

DISCUSSION

Evaluation of Intracellular ROS Formation in MCF-7 Cells

Intracellular ROS generation during treatment was estimated using fluorescence emission of DCF at 520 nm. In this article, DCFH-DA passively entered the cells and was deacetylated to non-fluorescent DCFH by esterases. Upon interaction of intracellular ROS with DCFH, DCF was produced. Figure 7 shows the MCF-7 intracellular ROS levels upon treatment with laser light (P^+), US waves (S^+), laser light/US waves (P^+S^+), Au-PoAP NC (NC^+), doxorubicin (Dox^+), Au-PoAP NC with doxorubicin

[DOI: 10.61186/mci.7.3.9]

(NC^+Dox^+), Au-PoAP NC upon PTT (NC^+P^+), SDT (NC^+S^+), and PTT/SDT ($NC^+P^+S^+$), doxorubicin upon PTT (Dox^+P^+), SDT (Dox^+S^+) and PTT/SDT ($Dox^+P^+S^+$), and Au-PoAP NC with doxorubicin upon PTT (NC^+Dox^+P+), SDT (NC^+Dox^+S+), and PTT/SDT ($NC^+Dox^+P^+S^+$). Without Au-PoAP NC and doxorubicin, compared to light irradiation, the ROS level generated in the S^+ group was more than the P^+ one, indicating that US exposure has a greater capacity to generate ROS. Compared to the results obtained from the MTT assay, it can be deduced that although more ROS was generated from US exposure, thermal effects from light irradiation played a more impressive role in eradicating cancerous cells. Like MTT article results, the level of generated ROS for the P^+S^+ group (synchronous light irradiation and US exposure) was greater than both P^+ and S^+ groups, with a significant difference and a synergistic value. Therefore, synchronous light irradiation and US exposure had a synergism effect to produce ROS. Figure 7 also indicates that light irradiation and US exposure alone or synchronously generated little ROS amounts. The combination of Au-PoAP NC and/or doxorubicin resulted in increased levels of reactive oxygen species (ROS) compared to the P^+, S^+, and P^+S^+ groups. The highest ROS levels were observed in the $NC^+Dox^+P^+S^+$ group, utilizing a combination of light irradiation and US exposure with both Au-PoAP NC and doxorubicin. These results are in line with the toxicity evaluation in MTT assay. The results also implied that both Au-PoAP NC and doxorubicin are ROS generators, and from this aspect, Au-PoAP NC acts as a chemotherapeutic agent. On the other hand, light irradiation and US exposure in the presence of either Au-PoAP NC or doxorubicin generated ROS in synergism manners, i.e., ROS level for Dox^+S^+ was higher than both and summation of Dox^+ and S^+, for NC^+P^+ was higher than both and summation of NC^+ and P^+, for Dox^+P^+ was higher than both and summation of Dox^+ and P^+, and for NC^+S^+ was higher than both and summation of NC^+ and S^+. They are matched with the data obtained from the cell toxicity assay. It seems that in terms of ROS generation ability, both Au-PoAP NC and doxorubicin are activated by both light irradiation and US exposure, and Au-PoAP NC and doxorubicin act as powerful photo/sonosensitizer. Moreover, both Au-PoAP NC and doxorubicin generated higher ROS levels when activated by US exposure, compared to activation by light irradiation. These deductions are in contrast with the MTT assay results and can be related to thermal effects from light irradiation. A consistent result was also obtained when Au-PoAP NC with doxorubicin was activated by US exposure. It can be inferred that the sonosensitizing ability of Au-PoAP NC and doxorubicin was more than their photosensitizing ability from the aspect of ROS generation. The photo/sonosensitizing ability of doxorubicin was rarely reported elsewhere [51]. Ultimately, in line with MTT assay results, the highest level of ROS was generated by the cumulative effect of Au-PoAP NC with doxorubicin upon PTT and SDT. The generation of heat upon PTT induces apoptosis [52], and the generation of ROS causes damage to the mitochondrial membrane by inducing lipid peroxidation [50]. Moreover, synchronous PTT/SDT causes depolarization of mitochondrial membrane potential, causing mitochondrial membrane leakage to increase against the penetration of chemotherapeutic drugs (facilitated chemotherapeutic drug delivery) [53].

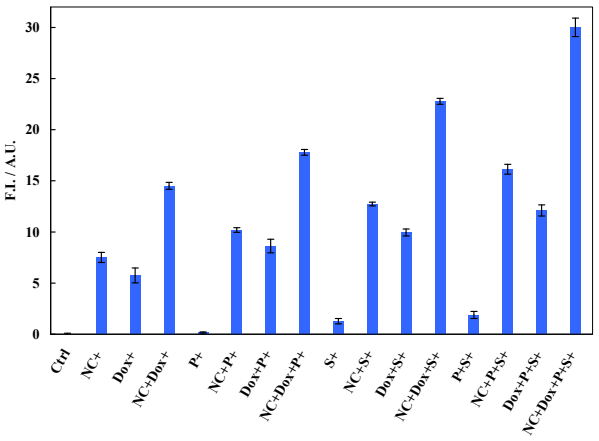

Figure 7: F.I.s of MCF-7 cells as indicators of intracellular ROS levels upon treatment with laser light (P^+), US waves (S^+), laser light/US waves (P^+S^+), Au-PoAP NC of 5 μg mL^{-1} (NC^+), doxorubicin of 0.58 μg mL^{-1} (Dox^+), Au-PoAP NC of 5 μg mL^{-1} with doxorubicin of 0.58 μg mL^{-1} (NC^+Dox^+), Au-PoAP NC of 5 μg mL^{-1} upon PTT (NC^+P^+), SDT (NC^+S^+) and PTT/SDT ($NC^+P^+S^+$), doxorubicin of 0.58 μg mL^{-1} upon PTT (Dox^+P^+), SDT (Dox^+S^+) and PTT/SDT ($Dox^+P^+S^+$), and Au-PoAP NC of 5 μg mL^{-1} with doxorubicin of 0.58 μg mL^{-1} upon PTT ($NC^+Dox^+P^+$), SDT ($NC^+Dox^+S^+$) and PTT/SDT ($NC^+Dox^+P^+S^+$)

This study introduced Au-PoAP NC as a synergistic therapeutic agent for cancer cell treatment and dual sensitizer in PTT and SDT. While Au-PoAP NC and doxorubicin have separately produced effective cytotoxicity, this study showed that the

[DOI: 10.61186/mci.7.3.9]

combination of these two agents resulted in an efficient annihilation of the MCF-7 cell line. Au-PoAP NC represented an efficient dual photo/sonosensitizer activity upon irradiation by 808 nm light and/or exposure by US waves. Radiation of doxorubicin by these two energy sources also led to deeper effectiveness and introduced a new route of facilitated doxorubicin delivery. Intercellular ROS generation was one of the main mechanisms of cell toxicity that was accelerated to the highest level using Au-PoAP NC with doxorubicin upon PTT/SDT. The pathway of high levels of ROS production and cell death induction went through synergism effects of the treatment components, i.e., radiations and chemicals.

ACKNOWLEDGMENTS

None Declared.

CONFLICT OF INTEREST

The authors have no conflict of interest.

ETHICS APPROVAL

This study was extracted from P. Tamaddon's M.Sc. thesis supported by the Research Council of Shiraz University of Medical Sciences (25509) with IR.SUMS.REC.1401.124 Ethics ID.

REFERENCE

1. Hausman DM. What Is Cancer? Perspect Biol Med. 2019;62(4):778-84. DOI: 10.1353/pbm.2019.0046 PMID: 31761807.
2. Sun YS, Zhao Z, Yang ZN, Xu F, Lu HJ, Zhu ZY, et al. Risk Factors and Preventions of Breast Cancer. Int J Biol Sci. 2017;13(11):1387-97. DOI: 10.7150/ijbs.21635 PMID: 29209143.
3. Haume K, Rosa S, Grellet S, Smialek MA, Butterworth KT, Solov'yov AV, et al. Gold nanoparticles for cancer radiotherapy: a review. Cancer Nanotechnol. 2016;7(1):8. DOI: 10.1186/s12645-016-0021-x PMID: 27867425.
4. Wyld L, Audisio RA, Poston GJ. The evolution of cancer surgery and future perspectives. Nat Rev Clin Oncol. 2015;12(2):115-24. DOI: 10.1038/nrclinonc.2014.191 PMID: 25384943.
5. Deng GL, Zeng S, Shen H. Chemotherapy and target therapy for hepatocellular carcinoma: New advances and challenges. World J Hepatol. 2015;7(5):787-98. DOI: 10.4254/wjh.v7.i5.787 PMID: 25914779.
6. Kim HS, Lee DY. Near-Infrared-Responsive Cancer Photothermal and Photodynamic Therapy Using Gold Nanoparticles. Polymers (Basel). 2018;10(9). DOI: 10.3390/polym10090961 PMID: 30960886.
7. Tachibana K, Feril LB, Jr., Ikeda-Dantsuji Y. Sonodynamic therapy. Ultrasonics. 2008;48(4):253-9. DOI: 10.1016/j.ultras.2008.02.003 PMID: 18433819.
8. Yu T, Wang Z, Mason TJ. A review of research into the uses of low level ultrasound in cancer therapy. Ultrason Sonochem. 2004;11(2):95-103. DOI: 10.1016/S1350-4177(03)00157-3 PMID: 15030786.
9. Rosenthal I, Sostaric JZ, Riesz P. Sonodynamic therapy--a review of the synergistic effects of drugs and ultrasound. Ultrason Sonochem. 2004;11(6):349-63. DOI: 10.1016/j.ultsonch.2004.03.004 PMID: 15302020.
10. Canavese G, Ancona A, Racca L, Canta M, Dumontel B, Barbaresco F, et al. Nanoparticle-assisted ultrasound: A special focus on sonodynamic therapy against cancer. Chem Eng J. 2018;340:155-72. DOI: 10.1016/j.cej.2018.01.060 PMID: 30881202.
11. McHale AP, Callan JF, Nomikou N, Fowley C, Callan B. Sonodynamic Therapy: Concept, Mechanism and Application to Cancer Treatment. Adv Exp Med Biol. 2016;880:429-50. DOI: 10.1007/978-3-319-22536-4_22 PMID: 26486350.
12. Wang P, Wang X, Ma L, Sahi S, Li L, Wang X, et al. Nanosonosensitization by Using Copper–Cysteamine Nanoparticles Augmented Sonodynamic Cancer Treatment. Part Part Syst Charact. 2018;35(4):1700378. DOI: https://doi.org/10.1002/ppsc.201700378.
13. Yang Z, Yao J, Wang J, Zhang C, Cao Y, Hao L, et al. Ferrite-encapsulated nanoparticles with stable photothermal performance for multimodal imaging-guided atherosclerotic plaque neovascularization therapy. Biomater Sci. 2021;9(16):5652-64. DOI: 10.1039/d1bm00343g PMID: 34259244.
14. Yao J, Yang Z, Huang L, Yang C, Wang J, Cao Y, et al. Low-Intensity Focused Ultrasound-Responsive Ferrite-Encapsulated Nanoparticles for Atherosclerotic Plaque Neovascularization Theranostics. Adv Sci (Weinh). 2021;8(19):e2100850. DOI: 10.1002/advs.202100850 PMID: 34382370.
15. Bernard V, Mornstein V, Jaroš J, Sedláčková M, Škorpíková J. Combined effect of silver nanoparticles and therapeutical ultrasound on ovarian carcinoma cells A2780. J Appl Biomed. 2014;12(3):137-45.
16. Boca SC, Potara M, Gabudean AM, Juhem A, Baldeck PL, Astilean S. Chitosan-coated triangular silver nanoparticles as a novel class of biocompatible, highly effective photothermal transducers for in vitro cancer cell therapy. Cancer Lett. 2011;311(2):131-40. DOI: 10.1016/j.canlet.2011.06.022 PMID: 21840122.
17. Wang T, Zhang L, Su Z, Wang C, Liao Y, Fu Q. Multifunctional hollow mesoporous silica nanocages for cancer cell detection and the combined chemotherapy and photodynamic therapy. ACS Appl Mater Interfaces. 2011;3(7):2479-86. DOI: 10.1021/am200364e PMID: 21604817.
18. Wang J, Jiao Y, Shao Y. Mesoporous Silica Nanoparticles for Dual-Mode Chemo-Sonodynamic Therapy by Low-Energy Ultrasound. Materials (Basel). 2018;11(10). DOI: 10.3390/ma11102041 PMID: 30347751.

19. Ou G, Li Z, Li D, Cheng L, Liu Z, Wu H. Photothermal therapy by using titanium oxide nanoparticles. Nano Res. 2016;9(5):1236-43. DOI: 10.1007/s12274-016-1019-8.
20. Ninomiya K, Noda K, Ogino C, Kuroda S, Shimizu N. Enhanced OH radical generation by dual-frequency ultrasound with TiO2 nanoparticles: its application to targeted sonodynamic therapy. Ultrason Sonochem. 2014;21(1):289-94. DOI: 10.1016/j.ultsonch.2013.05.005 PMID: 23746399.
21. Dai ZJ, Li S, Gao J, Xu XN, Lu WF, Lin S, et al. Sonodynamic therapy (SDT): a novel treatment of cancer based on sonosensitizer liposome as a new drug carrier. Med Hypotheses. 2013;80(3):300-2. DOI: 10.1016/j.mehy.2012.12.009 PMID: 23294609.
22. Anilkumar TS, Lu Y-J, Chen H-A, Hsu H-L, Jose G, Chen J-P. Dual targeted magnetic photosensitive liposomes for photothermal/photodynamic tumor therapy. J Magn Magn Mater. 2019;473:241-52. DOI: https://doi.org/10.1016/j.jmmm.2018.10.020.
23. Heli H, Rahi A. Synthesis and Applications of Nanoflowers. Recent Pat Nanotechnol. 2016;10(2):86-115. DOI: 10.2174/1872210510999160517102102 PMID: 27502388.
24. Yang W, Liang H, Ma S, Wang D, Huang J. Gold nanoparticle based photothermal therapy: Development and application for effective cancer treatment. Sustain Mater Technol. 2019;22:e00109. DOI: https://doi.org/10.1016/j.susmat.2019.e00109.
25. Negahdary M, Heli H. An electrochemical peptide-based biosensor for the Alzheimer biomarker amyloid-beta((1-42)) using a microporous gold nanostructure. Mikrochim Acta. 2019;186(12):766. DOI: 10.1007/s00604-019-3903-x PMID: 31713687.
26. Sheth RA, Wen X, Li J, Melancon MP, Ji X, Wang YA, et al. Doxorubicin-loaded hollow gold nanospheres for dual photothermal ablation and chemoembolization therapy. Cancer Nanotechnol. 2020;11(1). DOI: 10.1186/s12645-020-00062-8 PMID: 34335988.
27. Kayani Z, Dehdari Vais R, Soratijahromi E, Mohammadi S, Sattarahmady N. Curcumin-gold-polyethylene glycol nanoparticles as a nanosensitizer for photothermal and sonodynamic therapies: In vitro and animal model studies. Photodiagnosis Photodyn Ther. 2021;33:102139. DOI: 10.1016/j.pdpdt.2020.102139 PMID: 33310015.
28. Brazzale C, Canaparo R, Racca L, Foglietta F, Durando G, Fantozzi R, et al. Enhanced selective sonosensitizing efficacy of ultrasound-based anticancer treatment by targeted gold nanoparticles. Nanomedicine (Lond). 2016;11(23):3053-70. DOI: 10.2217/nnm-2016-0293 PMID: 27627904.
29. Chandran SP, Natarajan SB, Chandraseharan S, Mohd Shahimi MSB. Nano drug delivery strategy of 5-fluorouracil for the treatment of colorectal cancer. J Cancer Res Pract. 2017;4(2):45-8. DOI: https://doi.org/10.1016/j.jcrpr.2017.02.002.
30. Ding Y, Zhou YY, Chen H, Geng DD, Wu DY, Hong J, et al. The performance of thiol-terminated PEG-paclitaxel-conjugated gold nanoparticles. Biomaterials. 2013;34(38):10217-27. DOI: 10.1016/j.biomaterials.2013.09.008 PMID: 24055524.
31. Kim DH, Martin DC. Sustained release of dexamethasone from hydrophilic matrices using PLGA nanoparticles for neural drug delivery. Biomaterials. 2006;27(15):3031-7. DOI: 10.1016/j.biomaterials.2005.12.021 PMID: 16443270.
32. Rahi A, Sattarahmady N, Dehdari Vais R, Heli H. Sonoelectrodeposition of gold nanorods at a gold surface – Application for electrocatalytic reduction and determination of nitrofurazone. Sens Actuators B Chem. 2015;210:96-102. DOI: https://doi.org/10.1016/j.snb.2014.12.090.
33. Feng J, Gao J, Yang W, Liu R, Shafi M, Zha Z, et al. LSPR optical fiber sensor based on 3D gold nanoparticles with monolayer graphene as a spacer. Opt Express. 2022;30(6):10187-98. DOI: 10.1364/OE.453806 PMID: 35299428.
34. Wang L, Liu N, Ma Z. Novel gold-decorated polyaniline derivatives as redox-active species for simultaneous detection of three biomarkers of lung cancer. J Mater Chem B. 2015;3(14):2867-72. DOI: 10.1039/c5tb00001g PMID: 32262415.
35. Negahdary M, Heli H. An ultrasensitive electrochemical aptasensor for early diagnosis of Alzheimer's disease, using a fern leaves-like gold nanostructure. Talanta. 2019;198:510-7. DOI: 10.1016/j.talanta.2019.01.109 PMID: 30876593.
36. Wang X, Teng Z, Wang H, Wang C, Liu Y, Tang Y, et al. Increasing the cytotoxicity of doxorubicin in breast cancer MCF-7 cells with multidrug resistance using a mesoporous silica nanoparticle drug delivery system. Int J Clin Exp Pathol. 2014;7(4):1337-47. PMID: 24817930.
37. Pantshwa JM, Kondiah PPD, Choonara YE, Marimuthu T, Pillay V. Nanodrug Delivery Systems for the Treatment of Ovarian Cancer. Cancers (Basel). 2020;12(1). DOI: 10.3390/cancers12010213 PMID: 31952210.
38. Hong Y, Che S, Hui B, Yang Y, Wang X, Zhang X, et al. Lung cancer therapy using doxorubicin and curcumin combination: Targeted prodrug based, pH sensitive nanomedicine. Biomed Pharmacother. 2019;112:108614. DOI: 10.1016/j.biopha.2019.108614 PMID: 30798129.
39. Salapa J, Bushman A, Lowe K, Irudayaraj J. Nano drug delivery systems in upper gastrointestinal cancer therapy. Nano Converg. 2020;7(1):38. DOI: 10.1186/s40580-020-00247-2 PMID: 33301056.
40. Li S, Zhang D, Sheng S, Sun H. Targeting thyroid cancer with acid-triggered release of doxorubicin from silicon dioxide nanoparticles. Int J Nanomedicine. 2017;12:5993-6003. DOI: 10.2147/IJN.S137335 PMID: 28860762.
41. van der Zanden SY, Qiao X, Neefjes J. New insights into the activities and toxicities of the old anticancer drug doxorubicin. FEBS J. 2021;288(21):6095-111. DOI: 10.1111/febs.15583 PMID: 33022843.
42. Carvalho C, Santos RX, Cardoso S, Correia S, Oliveira PJ, Santos MS, et al. Doxorubicin: the good, the bad and the ugly effect. Curr Med Chem. 2009;16(25):3267-85. DOI: 10.2174/092986709788803312 PMID: 19548866.
43. Roell KR, Reif DM, Motsinger-Reif AA. An Introduction to Terminology and Methodology of Chemical Synergy-Perspectives from Across Disciplines. Front Pharma-

col. 2017;8:158. DOI: 10.3389/fphar.2017.00158 PMID: 28473769.

44. Foucquier J, Guedj M. Analysis of drug combinations: current methodological landscape. Pharmacol Res Perspect. 2015;3(3):e00149. DOI: 10.1002/prp2.149 PMID: 26171228.
45. Huo S, Ma H, Huang K, Liu J, Wei T, Jin S, et al. Superior penetration and retention behavior of 50 nm gold nanoparticles in tumors. Cancer Res. 2013;73(1):319-30. DOI: 10.1158/0008-5472.CAN-12-2071 PMID: 23074284.
46. Otsuka H, Nagasaki Y, Kataoka K. PEGylated nanoparticles for biological and pharmaceutical applications. Adv Drug Deliv Rev. 2003;55(3):403-19. DOI: 10.1016/s0169-409x(02)00226-0 PMID: 12628324.
47. Jiang Q, Liu Y, Guo R, Yao X, Sung S, Pang Z, et al. Erythrocyte-cancer hybrid membrane-camouflaged melanin nanoparticles for enhancing photothermal therapy efficacy in tumors. Biomaterials. 2019;192:292-308. DOI: 10.1016/j.biomaterials.2018.11.021 PMID: 30465973.
48. Fang XJ, Jiang H, Zhu YQ, Zhang LY, Fan QH, Tian Y. Doxorubicin induces drug resistance and expression of the novel CD44st via NF-kappaB in human breast cancer MCF-7 cells. Oncol Rep. 2014;31(6):2735-42. DOI: 10.3892/or.2014.3131 PMID: 24715151.
49. Wu BB, Leung KT, Poon EN. Mitochondrial-Targeted Therapy for Doxorubicin-Induced Cardiotoxicity. Int J Mol Sci. 2022;23(3). DOI: 10.3390/ijms23031912 PMID: 35163838.
50. Jackson TL. Intracellular accumulation and mechanism of action of doxorubicin in a spatio-temporal tumor model. J Theor Biol. 2003;220(2):201-13. DOI: 10.1006/jtbi.2003.3156 PMID: 12468292.
51. Yoshida T, Kondo T, Ogawa R, Feril LB, Jr., Zhao QL, Watanabe A, et al. Combination of doxorubicin and low-intensity ultrasound causes a synergistic enhancement in cell killing and an additive enhancement in apoptosis induction in human lymphoma U937 cells. Cancer Chemother Pharmacol. 2008;61(4):559-67. DOI: 10.1007/s00280-007-0503-y PMID: 17505825.
52. Melamed JR, Edelstein RS, Day ES. Elucidating the fundamental mechanisms of cell death triggered by photothermal therapy. ACS Nano. 2015;9(1):6-11. DOI: 10.1021/acsnano.5b00021 PMID: 25590560.
53. Wang X, Liu Y, Liu T, Mustafa F, Guan Q. Doxorubicin and Zinc phthalocyanine loaded pH-responsive FA-BSP-SA/TPGS micelles for synergistic chemo-photodynamic therapy against tumors. J Drug Deliv Sci Technol. 2022;76:103713. DOI: 10.1016/j.jddst.2022.103713.